Preprints of the 21st IFAC World Congress (Virtual)
Berlin, Germany, July 12-17, 2020

On the Fear of Falling Detection by Moving Horizon Estimation ⋆

Hedyeh Jafari * **Sina Sharif Mansouri** *
George Nikolakopoulos * **Thomas Gustafsson** *

* *Control Engineering and Robotic Teams at Luleå University of Technology, Luleå, Sweden (e-mail: hedjaf@ltu.se)*

Abstract: Fear of falling (FoF) is a major health problem, especially in elders, which can lead to falls, injury, loss of independence, and premature needs of nursing and assistance. However, most of the studies have focused on the psychological aspect of the FoF and there is a significant lack of technological assistance and methodology to detect and eliminate the effects of this fear on maintaining balance. In this article, we propose a novel method to detect the FoF as a quantitative signal. In our proposed novel approach, fear is considered as an internal disturbance inside a Central Nervous System (CNS) that can affect the generated output torque to each joint of the psychical body. By assuming the human body in a quiet stance, as an inverted pendulum model, this disturbance signal is estimated by Moving Horizon Estimation (MHE). For this purpose, the body kinetics and kinematics measurements of forty-five subjects during upright stance trails, as well as the psychological FoF falls efficacy test, were collected and utilized for the estimation and validation of the results. The experimental results show that the subjects with FoF present a higher variation in the estimated signal. This method can sufficiently detect the FoF by the posturographic and motion data, which can be utilized on the future assistive devices for prevention and treatment of the FoF and falls.

Keywords: Fear Estimation, Biomedical System, Quantification of physiological parameters for diagnosis and treatment assessment, Balance, Estimation.

1. INTRODUCTION

Basophobia or the Fear of falling (FoF) is a feeling related to the risk of falling that is not necessarily a psychological result of a fall (Trombetti et al., 2016), while aging and decline in the postural and musculoskeletal systems can increase the prevalence of this fear (Scheffer et al., 2008). Nowadays, the FoF is a significant predictor of falls, while in the community-dwelling, older adults who suffer from FoF, are more likely to fall (O and El Fakiri, 2015). Furthermore, FoF contribute to limited mobility and activities, decline of social interactions that might cause loss of independence and need for admission into nursing homes (Stubbs et al., 2014). Since life expectancy and the number of older adults is increasing worldwide, FoF is a major clinical and public health problem that needs considerable attention.

Until now, the diagnosis of FoF has been considered in many studies (Scheffer et al., 2008). Falls Efficacy Scale (FES) and a modified version, Falls Efficacy Scale-International (FES-I), are the most popular tests to detect the fall-related concern during daily psychical and social activities (Tinetti et al., 1990). In fact, these tests are mostly questionnaires that evaluate the self-efficacy to perform daily activities without a balance problem. In (Dueñas et al., 2016), the authors used posturography of the subjects in a standing position and found a significant relationship between some of the posturographic parameters and fall risk factors, such as FoF. Despite this current interest, and to the best of our knowledge, there have been no attempts to develop methods measuring fear as a quantitative value.

On the other hand, in the motor control field of studies, in the human balance system, the Central Nervous System (CNS) as the main controller, receives information from different modalities of the sensory system such as visual, vestibular, and proprioception in a closed feedback loop. Based on the integration of these data, it sends the proper motor command to the musculoskeletal system to stabilize the body (Horak, 2006; Chiba et al., 2016). However, any internal or external disturbances can affect the performance of the human balance system and result in a fall. Also, fear is a chain reaction that occurs in the brain startings with stimuli and endings with the release of chemicals (Kalin, 1993). Therefore, it can be assumed that FoF is an internal disturbance inside the nervous system that increases the error in the motor command and can be estimated by state estimation methods in control theory.

Moving Horizon Estimation (MHE) like other state estimation, can rebuild the full states of the system from noisy measurements as well as the overall model of the system (Haseltine and Rawlings, 2005). External forces or disturbances can be also assumed as states of the system. MHE can solve the estimation problem as an online optimization problem and it is able to handle complex nonlinear dynamic models and inequality constraints (Rao, 2000;

⋆ This work was funded by the Swedish Research Council Office under the Grant Agreement No.K2015-99X-22756-01-4.

Findeisen, 1997). Besides, since MHE considers the past measurements to estimate the current time, the estimation result is more robust against disturbances and delayed measurements (Ji et al., 2015). These advantages of MHE make it more attractive when compared to the classical state estimators, such as Kalman filter (KF) or Extended Kalman Filter (EKF). For the past decade, the computation time of the MHE optimization problem was an issue; however, with current solvers for nonlinear optimal control problems, such as Proximal Averaged Newton-type method for Optimal Control (PANOC), the MHE can be solved in real-time with high accuracy (Stella et al., 2017; Sathya et al., 2018).

This article proposes a new technical approach to detect the FoF by assuming it as an internal disturbance inside the CNS that is estimated by MHE. Within the framework of these criteria, the contribution of this work has three folds. First, to the best of our knowledge, it is the first attempt to detect FoF as a quantitative value from posturographic and motion data. Second, the FoF is considered as an internal disturbance inside the CNS which affect the generated torque to the joints of the human body. The human body in quiet stance, a posture in which the body's Center Of Mass (COM) is regulated around the ankle joint, is similar to an inverted pendulum model (Winter, 1995). Thus, this disturbance is estimated by the MHE through the PANOC solver. Finally, the methodology is validated by the most common psychological measurements FES-I and the subjects with high FES-I index have a significantly higher variation in the estimated signal. This shows the effectiveness of this method and provides initial works for a new way to diagnose and treat the FoF.

The rest of the article is structured as follows. Initially, the methodology is explained in Section 2, followed by an explanation of the human body model and the fast MHE. Section 3 describes the experimental protocol and the overall data collection for further validations. In Section 4, the simulation results are presented with proper discussion and analysis on the findings and finally in Section 5 the limitations are discussed with the corresponding perspectives for future work.

2. METHODOLOGY

The schematic of the human balance system is illustrated in Fig. 1. As it has been indicated, the CNS receives the feedback joints kinematics $(\theta, \dot{\theta})$, after the integration of multiple sensory organs, such as vestibular, vision and proprioception and transmits the proper motor commands (τ_j) to stabilize the body, while considering the joints intrinsic damping and stiffness (B_{pass}, K_{pass}). FoF can be assumed as a unit inside the CNS that generates disturbance torque (τ_f). This disturbance torque is later estimated by the MHE from the measured kinetics (τ_j) and kinematics (θ) of each individual subjects and the inverted model of the human body.

2.1 Inverted pendulum model

The human upright posture in anterior-posterior direction can be represented by a single link inverted pendulum

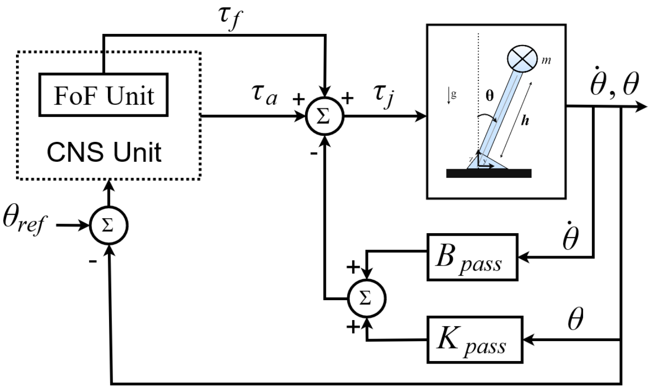

Fig. 1. The human balance scheme with the CNS as the main controller of the human body. The FoF is presented as block inside the CNS, which affects the generated torque τ_a.

around the ankle joint (Winter, 1995), while the dynamic equations of motion is described as:

$$J\ddot{\theta} = mgh \sin\theta - K\theta - B\dot{\theta} + \tau_a + \tau_f, \quad (1)$$

where $\theta \in \mathbb{R}$ and $\dot{\theta}$ are the angular position and angular velocity of the ankle, $m \in \mathbb{R}^+$ is the mass of the human body, $h \in \mathbb{R}^+$ is the distance between the center of mass and the ankle joint, $J \in \mathbb{R}^+$ is the moment of inertia of the body around the ankle, and g stands for the gravitational acceleration. The passive elements representing the inherent damping and stiffness of the ankle joint are presented by $B \in \mathbb{R}^+$ and $K \in \mathbb{R}^+$ respectively. The active torque, as an actuator of the system and corrector of the ankle joint, is represented by $\tau_a \in \mathbb{R}$, which is affected by the disturbance torque $\tau_f \in \mathbb{R}$. In this configuration, the states of the system are $X = [\theta, \dot{\theta}, \tau_f]^\top$, and the control input is $U = [\tau_j]$.

2.2 Moving horizon estimation

The equation of motion, described in Eq. (1), can be presented in the discrete time form as:

$$X_{k+1} = \mathcal{F}(X_k, U_k) + W_k, \quad (2a)$$

$$Y_k = \mathcal{H}(X_k) + \Lambda_k, \quad (2b)$$

where $\mathcal{F} : \mathbb{R}^{n_s} \times \mathbb{R}^{n_u} \to \mathbb{R}^{n_s}$ is a nonlinear function describing the dynamics of the system, $\mathcal{H} : \mathbb{R}^{n_s} \to \mathbb{R}^{n_m}$ is a linear vector function of the states X, and $Y = [\theta]$ is the measured output. The number of states, inputs and measurements are presented by n_s, n_u, n_m respectively. The measurement noise and model disturbances are presented by $\Lambda_k \in \mathbb{R}^{n_m}$ and $W_k \in \mathbb{R}^{n_s}$ respectively. It is assumed that the unknown process disturbance W_k, as well as the measurement noise Λ_k, are randomly distributed according to the Gaussian Probability Density Function (PDF) with the covariance matrix of $R \in \mathbb{R}^{n_m \times n_m}$ and $Q \in \mathbb{R}^{n_s \times n_s}$ (Ungarala, 2009). Furthermore, the prior information about the initial condition are assumed to be available and presented by $\bar{X}_0$. The initial PDF of the state vector is also assumed to be distributed according to the Gaussian PDF with the covariance matrix of $P \in \mathbb{R}^{n_s \times n_s}$. Based on the information about random noises, and a set of available noisy measurements $Y = \{Y_j : j = 1, ..., N_p\}$

and states of system $X = \{X_j : j = 0, ..., N_p\}$, MHE can be solved by the following optimization problem:

$$
\begin{aligned}
&\min_{X_{(k-N_p|k)}, W^{(k-1|k)}_{(k-N_p|k)}} \quad \mathrm{cost}(k) \\
&\text{s.t.} \\
&\quad X_{i+1|k} = \mathcal{F}(X_{i|k}, U_{i|k}) + W_{i|k} \\
&\quad Y_{i|k} = \mathcal{H}(X_{i|k}) + \Lambda_{i|k} \quad i = \{k - N_p, \dots k-1\} \\
&\quad W_k \in \mathbb{W}_k, \quad V_k \in \mathbb{V}_k, \quad x_k \in \mathbb{X}_k
\end{aligned} \tag{3}
$$

where,

$$
\begin{aligned}
\mathrm{cost}(k) = &\underbrace{\|X_{k-N_p|k} - \bar{X}_{k-N_p|k}\|^2_{P^{-1}}}_{\text{arrival cost}} \\
&+ \sum_{i=k-N_p}^{i=k} \underbrace{\|Y_{i|k} - \mathcal{H}(X_{i|k})\|^2_{R^{-1}}}_{\text{stage cost}} \\
&+ \sum_{i=k-N_p}^{i=k-1} \underbrace{\|X_{i+1|k} - \mathcal{F}(X_{i|k}, U_{i|k})\|^2_{Q^{-1}}}_{\text{stage cost}}
\end{aligned} \tag{4}
$$

In Eq. (3)-(4), $N_p \in \mathbb{N}$ is the size of the estimation window, $W^{(k-1|k)}_{(k-N_p|k)} = col(W_{(k-N_p|k)}, \dots, W_{(k-1|k)})$ are the estimated process disturbance from time $k - N_p$ up to $k-1$, estimated at time $k \in \mathbb{Z}^+$.

The first term of the objective function in Eq. (4), is called arrival cost and it is weighted by P, while it relates to the uncertainty in the initial states at the beginning of the horizon and it represents the error between the observation model and the the predicted initial state $\bar{X}(k - N_p \mid k)$. In other words, the arrival cost is the memory of the estimation that summarizes the information about the previous behavior of the system and the measurements up to the estimation window. The second and third terms are called stage cost with $\|Y_{i|k} - \mathcal{H}(X_{i|k})\|^2$, weighted by R, and it is the bias between the measured output and the estimated state and $\|X_{i+1|k} - \mathcal{F}(X_{i|k}, U_{i|k})\|$, weighted by Q, is the estimated model disturbance.

A corresponding estimated states and external forces of $X^\star_{k-N_p|k}, \cdots X^\star_{N_p|k}$ is obtained at each time instant from solving MHE optimization. The final estimated state $X^\star_{N_p|k}$ is used for further analyses. For the time less than the horizon window of size $k = \{0, \dots, N_p - 1\}$, and until the window is completed, the objective function is replaced by:

$$
\begin{aligned}
\mathrm{cost}(k) = &\|X_{0|k} - \bar{X}_{0|k}\|^2_{P^{-1}} \\
&+ \sum_{i=0}^{i=k} \|Y_{i|k} - \mathcal{H}(X_{i|k})\|^2_{R^{-1}} \\
&+ \sum_{i=0}^{i=k-1} \|X_{i+1|k} - \mathcal{F}(X_{i|k}, U_{i|k})))\|^2_{Q^{-1}}
\end{aligned} \tag{5}
$$

In this novel proposed scheme, the smoothing approach (Ungarala, 2009) is used for transferring the arrival cost term in Eq. (4), with only one time-step before the window is used for the arrival cost approximation. In fact, it is desired to use $X^\star_{(k-N_p)} = X^\star(k - N_p|k)$, including the measurements up to time $k - N_p$. Due to the shorter distance between the initial estimate and the desired estimate, the smoothing update leads to better performance in stability and convergence of MHE. The algorithm 1 presents an overview of implementation of the MHE.

Algorithm 1 The MHE algorithm.

Require: $P, Q, R, \bar{X}_0, N_p$;
while $k \le$ end time of simulation **do**
  if $k \le N_p$ **then**
    initialize $\{X_0, W_0\}$;
    solve the Eq. (5) and obtain $X^\star_k$;
  else
    Update $\{X_{k-N_p|k}, W^{(k-1|k)}_{(k-N_p|k)}\}$;
    Solve the MHE by Eq. (3)-(4), obtain $X^\star_k$;
    Save the last measurements;
    Move the horizon window;
  end if
  $k = k + 1$;
end while

Moreover, MHE is solved with PANOC (Sathya et al., 2018) with a single shooting formulation, where the gradient of objective function is obtained from automatic differentiation (Dunn and Bertsekas, 1989) in CasADi (Andersson et al., 2019). In general, PANOC combines projected-gradient updates with fast Newton-type directions by L-BFGS (Li and Fukushima, 2001), while it uses the Forward Backward Envelope (FBE) function. Due to the use of the FBE-based line search, from any initial guess PANOC converges globally. This algorithm can handle a large window size N_p and the MHE with dimension of $N_p \times ns$ decision variables, can be calculated approximately in real-time.

3. DATA COLLECTION

Forty-five healthy subjects, 27 women and 18 men, with mean age 75.2($\pm$4.5) years, mean height 167.2$(\pm 9.9)cm$, and mean weight 73.0$(\pm 12.2)kg$ participated in this study. The experiments were performed at the Human Health and Performance Lab at Luleå University of Technology, Luleå, Sweden. The study was executed in accordance with the Helsinki declaration and approved by the Regional Ethical Review Board in Umeå , Sweden (ref no. 2015-182-31). The acquired data is part of a larger project (Pauelsen et al., 2018; Jafari et al., 2018), where participants were recruited from a community in Northern Sweden.

The participants were asked to stand up straight, look at the dot on the wall and stand still as possible for $30s$. The kinetic data were measured by a force plate with a sampling frequency of 3000 Hz. The angular position of the joints was collected by a Qualisys motion Capture System with eight cameras and with a 200 Hz sampling rate. All data were synchronised through a stationary computer with the Qualisys Track Manager (QTM) software.

The FES was measured with the Falls Efficacy Scale-International, Swedish version FES-I, which is a questionnaire instrument with 16 items (Nordell et al., 2009). Each question has a Likert scale of 1 (not at all concerned) to 4 (very concerned). The results are indexed from 16 to 64, where 16 shows no concern and 64 presents that the subject is highly concerned of falling. The maximum score in the data set was 33 with a mean value of 21.

4. RESULTS

The parameter of the inverted pendulum model, such as J, m, and h are specified according to the measurements of each subject. The passive elements are set based on the average value determined in (Peterka, 2002) with the value of $B_{pass} = 57.29\ N.m.s.rad^{-1}$ and $K_{pass} = 85.94\ N.m.rad^{-1}$. Since in upright stance the body is swaying around the ankle, the ankle torque (τ_j) can be approximated from the force plate. Both the ankle torque (τ_j) and the ankle angular position (θ) signals of each subject are detrended to remove the sensors drifts. Subsequently, a high correlation between both signals, from the left and right joints of the body, of each subject, during the upright stance trails was observed. Therefore, only the right side of body joints were chosen for the estimation.

The horizon window of MHE N_p is set to 40, while the weights of the cost terms of MHE were set correspondingly as: ($P = 2 \times I^{3\times3}$, $Q = I^{3\times3}$, $R = I$) and I presents the Identity matrix. The results are obtained on a computer with an Intel Core i7-6600U CPU, 2.6GHz and 12GB RAM.

4.1 FoF estimation

Figure 2 presents the estimation results for two random subjects in the experimental data set. As it can be observed from the obtained results, the estimator can sufficiently estimate the measured angular position of the ankle's θ, the unknown states of the angular velocity $\dot{\theta}$ and the internal torque disturbance τ_f. The Root Mean Square Error (RMSE) of the estimation, for the measured angular positions for this two subjects, are 0.0007 *rad* and 0.0001 *rad*.

The computation time of the MHE, which is implemented in PANOC is provided in Fig. 3. In this case, the average computation time is 0.038 *sec*, which indicates the ability of the solver to solve the MHE with a large horizon window of $N_p = 40$.

Figure 4 depicts the estimation of the internal force τ_f for the subjects with the lowest concern of falling ($FES - I = 16$) and the subjects with higher concern of falling ($FES - I \geq 27$). It can be seen that for subjects with less score of fear, the estimation of this disturbance torque is almost zero, while for subjects with higher concern, this disturbance torque has more variation.

The comparison of Standard deviation (Std) of the estimated internal disturbance torque with the score of FES-I of all subjects in the data set is provided in Fig. 5. It can be observed that the Std of the disturbance torque τ_f for subjects with $FES - I \geq 24$ is higher than most of the subjects with $FES - I < 24$. Although there exist some outliers, the relation between the FES-I and the disturbance torque τ_f is roughly linear. However, by increasing the data samples, a precise mathematical model of this relation can be obtained as a future study.

4.2 Discussion

Quiet standing is usually considered as swaying around the ankle and is called "ankle strategy"; in which the ankle torque maintains the Center Of Mass (COM) over the base of support. By aging or in case of disturbances, other joints, such as hip, may involve to maintain the balance and prevent fall (Pollock et al., 2000). The "Hip strategy" is characterized by motion at the trunk, which causes the re-positioning of COM. However, how the brain decides to activate a joint or a combination of joints is still an open question (Karniel, 2011).

In this research article we study the effect of FoF on the variation of the ankle and hip joints of each subject by finding the ratio of the changes of Std of the angular

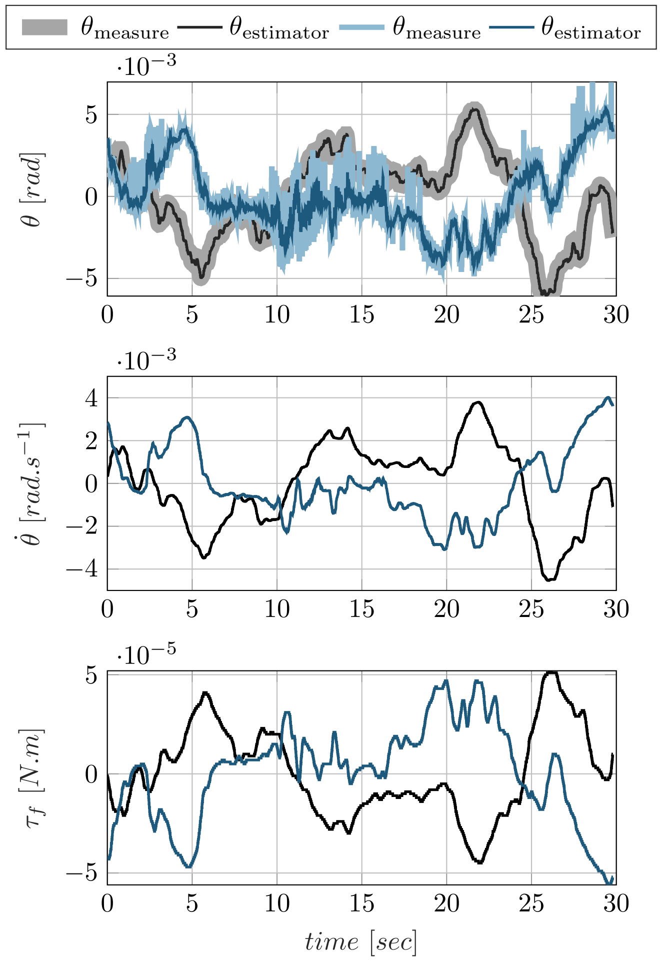

Fig. 2. Estimation of measured angular position of ankle θ, angular velocity $\dot{\theta}$ and internal torque disturbance τ_f for two random subjects, shown by blue and black color, in the data sets.

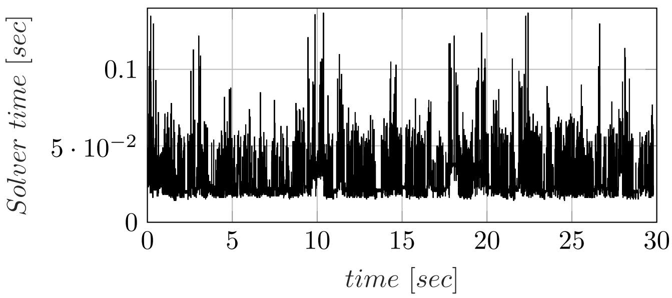

Fig. 3. The computation time of the solver.

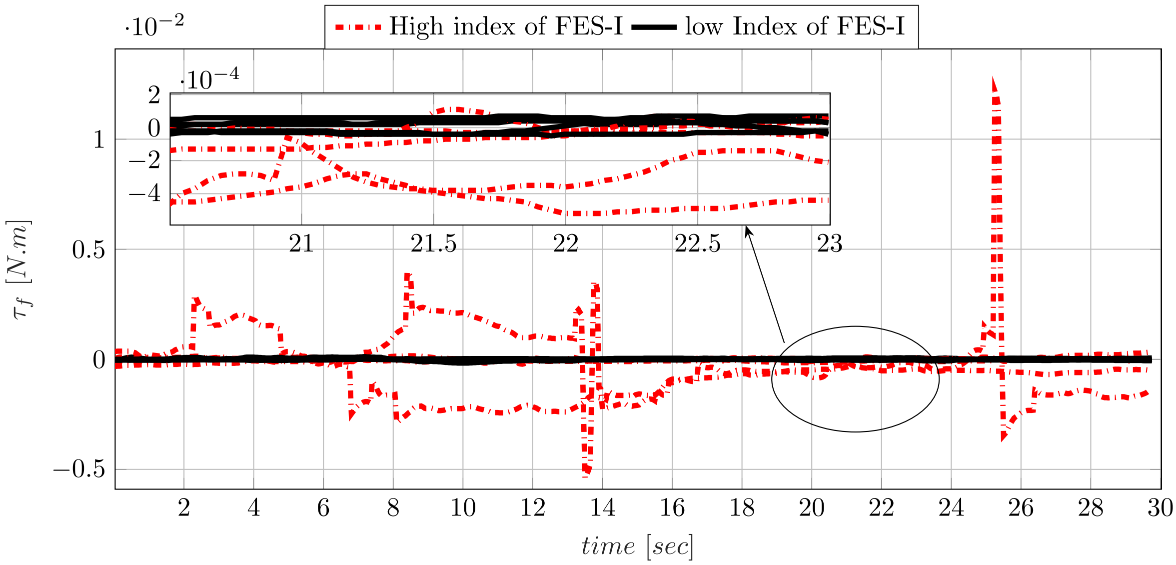

Fig. 4. Estimation of disturbance torque τ_f for subjects with extreme values for FES-I. The red Dash-dot lines show subjects with $FES-I \geq 27$ and solid black lines are subjects with $FES-I = 16$.

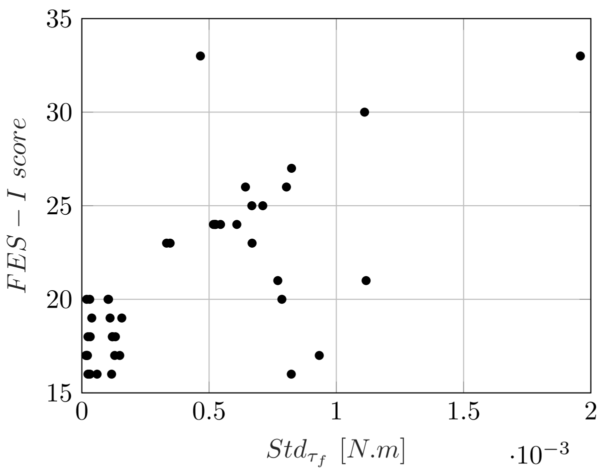

Fig. 5. Comparison of the FES-I score and the standard deviation (Std) of the estimated disturbance torque τ_f among all the subjects in the data set.

position of ankle joint (θ_{ankle}) and hip joint (θ_{hip}) as:

$$Ratio = Std_{ankle}/Std_{hip}. \tag{6}$$

Therefore, $Ratio \geq 1$ describes a higher variation in the ankle and represents the ankle strategy, while the $Ratio < 1$ can be assumed as a hip strategy.

Figure 6 shows the effect of FES-I score on the Std ratio. This figure reveals also that by increasing the concern and fear of falling, the majority of the subjects use the ankle strategy. However, the hip strategy is commonly used for the majority of subjects with a low score of FES-I. This reduced utilization of other joints in subjects with FoF, may be a result of the effect of fear and anxiety on the joint and muscle tension, while further conclusions in this direction are beyond the scope of this article and require further investigation.

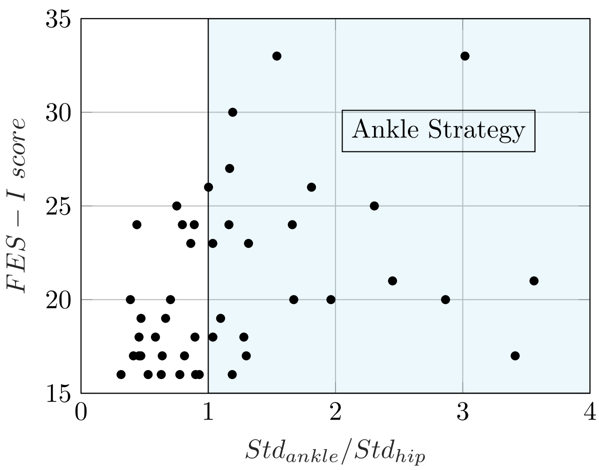

Fig. 6. The effect of FES-I score on the strategy of each subject to maintain balance. The horizontal axis presents the ratio of the standard deviation of the angular motion of the ankle joint to the hip joint. The blue shaded area shows the ankle strategy $ratio \geq 1$ and the white area illustrates the hip strategy.

5. CONCLUSION

In this article, a novel method to estimate FoF has been established, where the FoF can be considered as an internal disturbance inside the CNS. With the knowledge about the dynamics of the body and by measuring the angular position as the system output and the joint torque as a control output, this disturbance can be estimated by MHE through the fast solving of an optimal control problem PANOC. The results validate the performance of this estimation and indicate that a higher disturbance is applied to the joint torque to stabilize the body in people with a high concern of falling. This study can be investigated further, by a bigger sample size and in different age groups and other body postures, such as walking or stepping. This scientific results could be also a starting point towards the technical measurement of FoF that could eventually lead to the design of assistive devices for intervention and treatment of FoF.

REFERENCES

Andersson, J.A., Gillis, J., Horn, G., Rawlings, J.B., and Diehl, M. (2019). Casadi: a software framework for nonlinear optimization and optimal control. *Mathematical Programming Computation*, 11(1), 1–36.

Chiba, R., Takakusaki, K., Ota, J., Yozu, A., and Haga, N. (2016). Human upright posture control models based on multisensory inputs; in fast and slow dynamics. *Neuroscience research*, 104, 96–104.

Dueñas, L., i Bernat, M.B., del Horno, S.M., Aguilar-Rodriguez, M., and Alcántara, E. (2016). Development of predictive models for the estimation of the probability of suffering fear of falling and other fall risk factors based on posturography parameters in community-dwelling older adults. *International journal of industrial ergonomics*, 54, 131–138.

Dunn, J.C. and Bertsekas, D.P. (1989). Efficient dynamic programming implementations of newton's method for unconstrained optimal control problems. *Journal of Optimization Theory and Applications*, 63(1), 23–38.

Findeisen, P.K. (1997). *Moving horizon state estimation of discrete time systems*. Ph.D. thesis, University of Wisconsin–Madison.

Haseltine, E.L. and Rawlings, J.B. (2005). Critical evaluation of extended kalman filtering and moving-horizon estimation. *Industrial & engineering chemistry research*, 44(8), 2451–2460.

Horak, F.B. (2006). Postural orientation and equilibrium: what do we need to know about neural control of balance to prevent falls? *Age and ageing*, 35(suppl_2), ii7–ii11.

Jafari, H., Pauelsen, M., Röijezon, U., Nyberg, L., Nikolakopoulos, G., and Gustafsson, T. (2018). On internal modeling of the upright postural control in elderly. In *2018 IEEE International Conference on Robotics and Biomimetics (ROBIO)*, 231–236. IEEE.

Ji, L., Rawlings, J.B., Hu, W., Wynn, A., and Diehl, M. (2015). Robust stability of moving horizon estimation under bounded disturbances. *IEEE Transactions on Automatic Control*, 61(11), 3509–3514.

Kalin, N.H. (1993). The neurobiology of fear. *Scientific American*, 268(5), 94–101.

Karniel, A. (2011). Open questions in computational motor control. *Journal of integrative neuroscience*, 10(03), 385–411.

Li, D.H. and Fukushima, M. (2001). On the global convergence of the bfgs method for nonconvex unconstrained optimization problems. *SIAM Journal on Optimization*, 11(4), 1054–1064.

Nordell, E., Andreasson, M., Gall, K., and Thorngren, K.G. (2009). Evaluating the swedish version of the falls efficacy scale-international (fes-i). *Advances in Physiotherapy*, 11(2), 81–87.

O, Y.M. and El Fakiri, F. (2015). Gender differences in risk factors for single and recurrent falls among the community-dwelling elderly. *SAGE OPEN*, 5(3).

Pauelsen, M., Nyberg, L., Röijezon, U., and Vikman, I. (2018). Both psychological factors and physical performance are associated with fall-related concerns. *Aging clinical and experimental research*, 30(9), 1079–1085.

Peterka, R. (2002). Sensorimotor integration in human postural control. *Journal of neurophysiology*, 88(3), 1097–1118.

Pollock, A.S., Durward, B.R., Rowe, P.J., and Paul, J.P. (2000). What is balance? *Clinical rehabilitation*, 14(4), 402–406.

Rao, C.V. (2000). *Moving horizon strategies for the constrained monitoring and control of nonlinear discrete-time systems*. Ph.D. thesis, University of Wisconsin–Madison.

Sathya, A., Sopasakis, P., Van Parys, R., Themelis, A., Pipeleers, G., and Patrinos, P. (2018). Embedded nonlinear model predictive control for obstacle avoidance using panoc. In *2018 European Control Conference (ECC)*, 1523–1528. IEEE.

Scheffer, A.C., Schuurmans, M.J., Van Dijk, N., Van Der Hooft, T., and De Rooij, S.E. (2008). Fear of falling: measurement strategy, prevalence, risk factors and consequences among older persons. *Age and ageing*, 37(1), 19–24.

Stella, L., Themelis, A., Sopasakis, P., and Patrinos, P. (2017). A simple and efficient algorithm for nonlinear model predictive control. In *2017 IEEE 56th Annual Conference on Decision and Control (CDC)*, 1939–1944. IEEE.

Stubbs, B., West, E., Patchay, S., and Schofield, P. (2014). Is there a relationship between pain and psychological concerns related to falling in community dwelling older adults? a systematic review. *Disability and rehabilitation*, 36(23), 1931–1942.

Tinetti, M.E., Richman, D., and Powell, L. (1990). Falls efficacy as a measure of fear of falling. *Journal of gerontology*, 45(6), P239–P243.

Trombetti, A., Reid, K., Hars, M., Herrmann, F., Pasha, E., Phillips, E., and Fielding, R. (2016). Age-associated declines in muscle mass, strength, power, and physical performance: impact on fear of falling and quality of life. *Osteoporosis international*, 27(2), 463–471.

Ungarala, S. (2009). Computing arrival cost parameters in moving horizon estimation using sampling based filters. *Journal of Process Control*, 19(9), 1576–1588.

Winter, D.A. (1995). Human balance and posture control during standing and walking. *Gait & posture*, 3(4), 193–214.